Available online at www.sciencedirect.com

ScienceDirect

Procedia CIRP 141 (2026) 73–78

www.elsevier.com/locate/procedia

10th Conference on High Performance Cutting (CIRP-HPC 2026)

Mechanistic cutting force model: Identification of cutting coefficients in finish milling of polylactide (PLA) 3D-printed parts

Margaux Lorenzoni[a,*], Edouard Rivière-Lorphèvre[a], Laurent Spitaels[a], Jérémy Odent[b], François Ducobu[a]

[a]*Machine Design and Production Engineering Lab – Research Institute for Materials Science and Engineering, University of Mons, Place du Parc 20, 7000 Mons, Belgium*

[b]*Laboratory of Polymeric and Composite Materials (LMPC) – Center of Innovation and Research in Materials and Polymers (CIRMAP), University of Mons, Place du Parc 20, 7000 Mons, Belgium*

* Corresponding author. *E-mail address:* margaux.lorenzoni@umons.ac.be

Abstract

Finishing the parts obtained by Fused Filament Fabrication (FFF) is a promising approach to overcome its inherent limitations, such as poor surface roughness and dimensional accuracy. However, specific thermal properties of polymers, such as low melting temperature and low thermal conductivity, influence the cutting process and may, therefore, also affect the modeling of cutting forces. Unlike metals and composites, investigations into cutting forces models of polymers, including polylactide (PLA), are at a very early stage. Yet, these models have the potential to enhance the reliability of the polymer milling process. Furthermore, the use of finish milling on 3D-printed PLA parts is rising, particularly with the recent development of hybrid manufacturing machines, which increases the need for suitable cutting models. Therefore, this paper proposes to study a mechanistic model, as this type of model has shown a good compromise between simulation time and precision for other materials. The developed model is based on an inverse analysis to identify cutting coefficients from measured forces. Finish milling tests were conducted on PLA samples using various feed rates, cutting speeds and cutting fluid conditions. The identification of the cutting force model was performed on each sample individually then on the whole database using an iterative method. The good agreement between simulation and experiments in stable cutting conditions demonstrate the applicability of the model.

Keywords: Cutting forces; Milling; Mechanisitic model; Material extrusion, Polylactic acid; PLA

1. Introduction

Fused Filament Fabrication (FFF) is an additive manufacturing (AM) technology based on Material Extrusion (MEX) known for reducing the cost of customized parts with complex geometries [1]. However, despite being increasingly used for personalized production applications and prototyping, inherent limitations remain in terms of surface roughness of the final parts. A staircase effect, which refers to visibly offset layers, is often visible on 3D-printed parts as a result of the layer-by-layer building process [1,2].

To overcome such limitations, different post-processing techniques can be used [3]. One of them, namely finish milling, shows promising results as it allows to reach the best surface finish improvement among mechanical post-processing methods [3]. In addition, machining can either be performed after printing or in alternance with printing using a hybrid machine. The latter combines the additive and subtractive processes and therefore allows to benefit from the advantages of both technologies [4].

Among other thermoplastic polymers being used in MEX and hybrid manufacturing, Polylactide or Polylactic acid (PLA)

10.1016/j.procir.2026.03.049

is an interesting candidate for decreasing the environmental impact of the MEX process. This polymer can be biosourced [5] and, as for its end of life, it can be recycled as well as composted in the presence of micro-organisms [6].

Therefore, multiple research groups have recently started investigating PLA and its machinability, focusing on finish milling. Different approaches were taken, always focusing on reaching the best final surface quality: aiming to find the most suitable tools [7], the most compatible printing orientation [8], the most stable cutting forces measured during the machining process [9,10], and, overall, the most adapted milling parameters [8–12].

However, while most of these studies focus on cutting forces, models are not extensively discussed. Unlike models regarding machining of metallic materials [13] or fiber-reinforced polymeric matrix composites [14], cutting models for polymeric materials are not developed in the literature. A first approach was implemented by our own group [10] in a study focusing on the identification of optimized cutting parameters using the qualification test of the Couple Tool-Material standard NF E 66-520-6. The parameters of a mechanistic model, elaborated by Engin and Altintas [15] (initially for metallic materials), were identified on the data of the best cutting parameters case, by inverse analysis using Rivière-Lorphèvre and Filippi's method [16]. The model showed very good agreement with the experimental forces in this specific case. Therefore, this study aims to develop the mechanistic model for all the cutting conditions of the database and evaluate its applicability in the case of polymer machining.

2. Material and Method

2.1. Part design and printing

Cross-shaped parts (Fig. 1) were used to allow shoulder milling operations on the four sides of the sample without interference from previous operations. To ensure ease of printing, fillets of the nozzle diameter (0.4 mm) were used as recommended by Pei et al. [1].

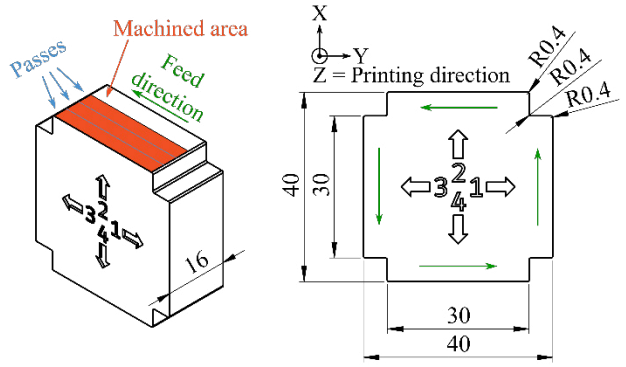

Fig. 1. Design of the parts in mm and definition of the passes, modified from Lorenzoni et al. [10].

These parts were printed using filament of Native Nanovia EF 3D850 Polylactic Acid (PLA) with a diameter of 2.85 mm. Before printing, the filament was dried for 16 hours, using a SUNLU FilaDryer S2. A level of 20% humidity was reached inside the drying device.

An Ultimaker S3 with AA 0.4 mm print cores was used to print the parts. Before each print, a light mist of 3DLAC adhesive spray was applied on the build plate to avoid sample warping. Printing parameters were chosen based on the Balanced Fast printing strategy of the Ultimaker Cura 5.6.0 slicer since the parts are meant to be finished by milling. A few parameters (Table 1) were modified to match the recommendations of the manufacturer.

Table 1. Modified printing parameters.

Printing parameter	Value
Wall thickness	5 mm
Top/Bottom pattern and thickness	Concentric, 1 mm
Infill pattern and density	Grid, 10%
Printing temperature	200°C
Printing speed	50 mm/s

2.2. Finish milling and cutting conditions

Finish milling operations were performed on a Mikron VCE 600 Pro, using a 93060-F solid end mill from Seco Tools. This tool was specifically designed by the manufacturer for thermoplastics and showed a diameter D of 6 mm, 2 teeth (Z), and a maximal axial depth of cut $a_{p,max}$ of 20 mm. A shoulder milling approach was used with a total of three consecutive passes on each sample side (Fig. 1). Each pass had an axial depth of cut a_p and a radial depth of cut a_e of 3 mm and 1 mm, respectively. When used, the cutting fluid was a compressed air flow at a 6-bar pressure. The tool did not show any sign of wear regarding ISO 8688-2 at the end of the experimental tests.

The starting cutting parameters were chosen from literature for giving the best results in terms of surface roughness after milling in dry conditions [9]. The parameters, given in terms of cutting speed v_c (in m/min) and feed per tooth f_z (in mm/tooth), then varied around their starting value by 20% following the experimental plan of Lorenzoni et al. [10]. The experimental plan (Table 2) was carried out twice: once using cutting fluid and once in dry conditions (without cutting fluid). Each set of cutting conditions was performed four times. Machining experiments were performed in conventional milling.

Table 2. Experimental plan.

Conditions category	v_c [m/min]	f_z [mm/tooth]
v_c-	60.3	0.1
f_z-	75.4	0.08
Baseline	75.4	0.1
f_z+	75.4	0.12
v_c+	90.5	0.1

2.3. Cutting forces

To record the cutting forces, the parts were linked to a Type 9256C2 Kistler force sensor using a 3D-printed support. Signals were acquired at a sampling frequency of 20 kHz and recorded thanks to a Kistler 5070A charge amplifier and a Kistler 5697A2 data acquisition system linked to a computer running the DynoWare software. The signal is postprocessed using a Butterworth low pass filter (4th order, cutoff frequency of 800 Hz) to remove the frequency content out of the bandwidth of the sensor. Additionally, the signal is processed to remove the part of the signal during which the tool is not cutting through the material as well as the transition parts corresponding to the tool entry and exit.

2.4. Mechanistic model

The paper explores the opportunity to model the cutting forces in PLA using a classical linear model developed for metal parts [15]. Two complementary approaches are taken in this study and evaluated in terms of performance with the same indicator. The first approach is referred to as local and computes the model on each file of the experimental dataset separately [16]. The second approach is introduced as global since the model is computed on the whole experimental database at once [17]. Both approaches are based on the same model which divides the cutter into slices along its axis (Fig. 2).

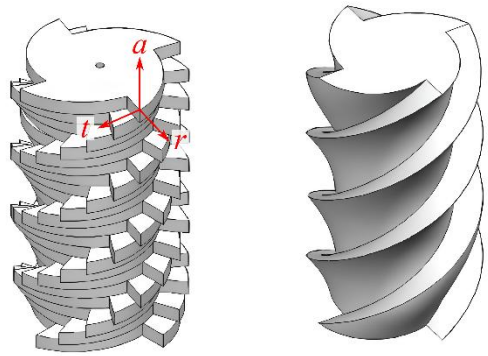

Fig. 2. Decomposition (left) of the endmill (right) in slices along its axis.

For each of these slices, the total cutting force is modeled in three components (*t*: tangential along cutting speed direction, *r*: radial along the local normal to the tool envelope and *a*: axial forming an orthogonal frame with *t* and *r*) computed as

$$dF_i = K_i \cdot h \cdot db \ (i = t, r, a) \tag{1}$$

with K_i the cutting forces coefficients (MPa), h the undeformed chip thickness (mm) and db the projected length of an infinitesimal cutting edge along the cutting speed direction (mm). These elementary forces are projected in a global frame (*x*: along feed direction, *z*: along the cutter axis and *y*: to form an orthogonal frame) and integrated along all cutting edges. The edge coefficients K_e were not considered in this work as it focuses on evaluating a simple model with a limited number of coefficients as a first approach on polymer modeling. Future work developing more complex models could include such coefficients.

The major drawback of this model is that the cutting forces coefficients are not directly linked to material properties such as yield strength or hardness for example. An identification procedure is then needed to obtain those values from experimental tests. In this paper, a method based on an inverse analysis is used in accordance with Rivière-Lorphèvre and Filippi's procedure [16]. For each time step, the equations linking the measured cutting force and the cutting force coefficient are established and assembled in a linear system

$$f = A \cdot k \tag{2}$$

with f the vector containing forces along *x*, *y* and *z* directions for each time steps, A a matrix taking into account the cutting force model and the projection matrix for the whole linear problem and k the vector containing the cutting forces coefficients. For the local approach, this overdetermined system is solved for each experimental test using the Moore Penrose pseudo inverse, minimizing the root mean square difference between simulated and measured forces

$$k = inv(A^T \cdot A) \cdot (A^T \cdot f) \tag{3}$$

Using the local approach, the cutting coefficients are therefore determined for each experimental test. The variation in computed cutting coefficient for identical cutting conditions allows to closely model the measured forces for each test.

On the other hand, to be able to get a predictive model, the global approach is used [17], and a set of specific pressures is extracted from the whole experimental database. Instead of solving the linear system for each case, the system is assembled in a global system gathering all experiments for all cutting tests. The assembled linear system to solve is constructed as

$$\begin{Bmatrix} f_1 \\ \vdots \\ f_n \end{Bmatrix} = \begin{bmatrix} A_1 \\ \vdots \\ A_n \end{bmatrix} \cdot k \tag{4}$$

with f_i the vector containing forces along *x*, *y* and *z* directions for each time steps for the ith experimental test, A_i the matrix taking into account the cutting force model and the projection matrix for the ith test and k the vector containing the cutting forces coefficients. The Moore Penrose pseudo inverse is again used to get the best average values of the cutting forces coefficients for the whole dataset. In this case, the computed coefficients are global and do not vary between experimental tests which allows to predict the cutting forces.

In summary, the two approaches are complementary with each other. The local approach allows to closely model each experiment with varying coefficients between tests measurements. The global approach adds a predictive aspect of the cutting forces values giving valuable insights about forces experienced by the workpiece during the milling process.

The indicator of performance (RMS) is the root mean square difference between measured and simulated cutting forces over one revolution of the cutter (according to Rivière-Lorphèvre and Filippi's method [16]) computed as

$$RMS = \sqrt{\frac{\sum_{i=1}^{n_{points}} \sum_{j=x,y,z} (F_{meas\ j,i} - F_{simulated\ j,i})^2}{n_{points}}} \quad (5)$$

with F_{meas} the measured cutting force and $F_{simulated}$ the simulated force, both projected on the axis j (j=x, y, z) of the global frame and summed over the n_{points} time steps.

3. Results and discussion

For a single cutting condition (local approach), the model is close to the experimental results with an RMS ranging from 1.82 to 3.70 N for all cutting conditions considered (Table 3). In comparison, the norm of the cutting force (including the contributions of F_x, F_y, and F_z) reaches a maximum of 40.24 N, with an average maximum of 33.55 N across all experimental tests. No significant difference can be observed between dry conditions and the conditions using cutting fluid. Fig. 3 and Fig. 4 show two examples of comparison between measured and modeled cutting forces for dry conditions and using cutting fluid, respectively.

Table 3. RMS between measured and modeled forces using the coefficients identified for a single experimental test (local) and the whole database (global).

	Dry conditions			With cutting fluid		
Conditions category	Max meas. force [N]	Local RMS [N]	Global RMS [N]	Max meas. force [N]	Local RMS [N]	Global RMS [N]
v_c-	38.80	2.97	5.16	37.58	3.30	4.63
	35.50	2.07	2.22	34.05	2.38	2.64
	35.23	2.70	3.09	37.87	3.70	4.83
	36.00	2.48	4.11	33.13	2.39	2.92
f_z-	31.09	2.85	4.14	31.44	2.99	4.27
	31.37	2.72	3.80	29.27	2.29	2.70
	28.78	2.82	3.24	33.52	3.35	5.04
	27.89	1.93	2.60	24.27	2.26	2.52
Baseline	34.20	2.61	2.91	37.77	3.55	4.78
	32.84	2.38	2.72	35.59	2.41	2.90
	37.12	2.37	4.77	32.61	3.48	3.75
	32.97	2.15	2.64	33.17	2.42	2.65
f_z+	18.46	2.34	15.93	34.79	2.45	4.16
	39.78	2.79	3.41	38.02	3.39	4.21
	40.24	2.72	3.16	36.73	3.24	3.56
	38.68	3.11	3.75	24.17	2.68	9.76
v_c+	37.20	2.10	3.40	33.12	2.75	2.96
	38.89	2.84	5.78	37.13	3.16	4.26
	35.85	2.74	2.98	34.60	2.44	2.61
	30.65	1.82	2.06	21.59	2.59	6.95

The analysis of the results shows that there is a significant range of variation of the cutting coefficients from one experimental test to another. K_t ranges from 73 to 237 MPa, K_r from 25 to 74 MPa and K_a from 27 to 105 MPa. Fig. 5 shows, for example, the tangential and radial cutting coefficients for all experimental tests in the database.

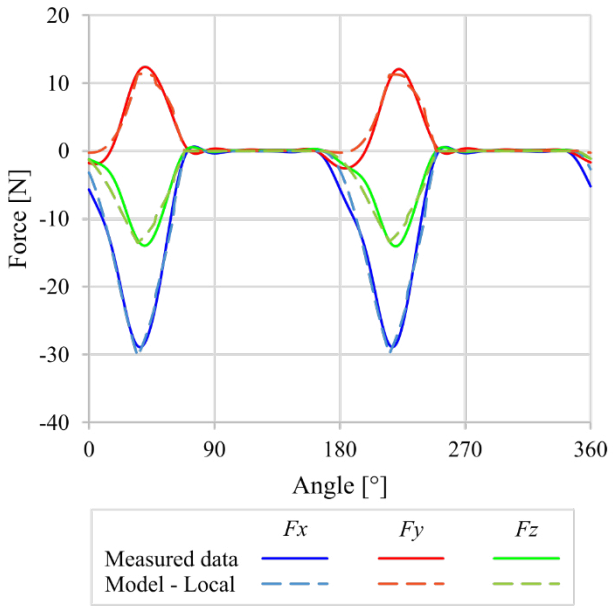

Fig. 3. Measured and modeled (local approach) cutting forces along x, y and z directions for the baseline case in dry conditions over one tool revolution.

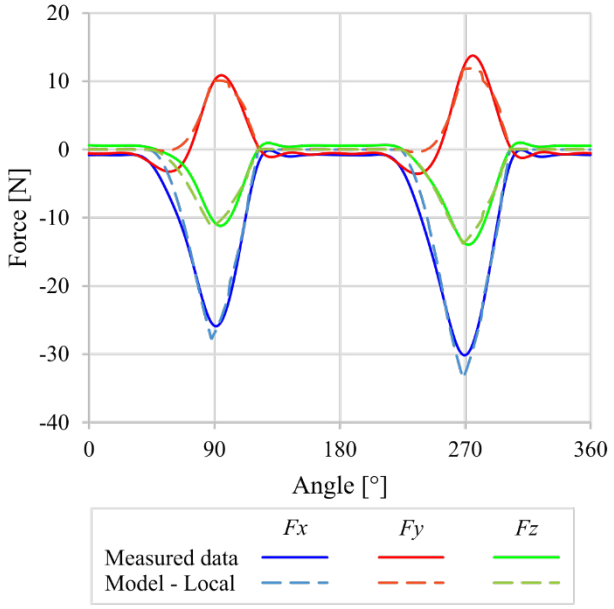

Fig. 4. Measured and modeled (local approach) cutting forces along x, y and z directions for the baseline case using cutting fluid over one tool revolution.

The variation in terms of coefficients between experimental tests may be due to the inverse analysis used to solve the system. For one experimental test, multiple sets of coefficients can coexist to model the test with the same accuracy. To avoid having such significant coefficients variations and, therefore, model variations, the global approach was used on the whole experimental database. For the global approach, the best average values of the specific cutting coefficients over the

whole dataset are K_t=190 MPa, K_r=49 MPa and K_a=83 MPa (Fig. 5).

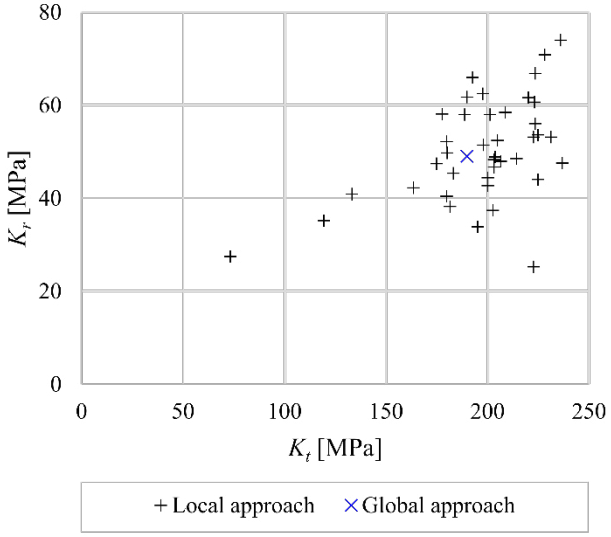

Fig. 5. Tangential and radial cutting coefficients for each experimental test.

Values from both global and local approaches can be compared to classic values for metallic materials. For instance, the cutting force coefficients vary from 1500 to 3500 MPa regarding K_t and from 2000 to 3200 MPa regarding K_r, using the same local and global approaches on machining of a titanium alloy [17]. In addition, cutting coefficients of 500 MPa and 200 MPa, for K_t and K_r respectively, were computed in aluminum alloy milling [18]. Therefore, some comments can be made:

- K_t is larger than K_r which is a general trend in metallic alloys as well;
- K_a coefficient is classically lower than K_t and K_r for metallic alloys, while being significantly higher than K_r for the PLA;
- The value of the cutting force coefficients is lower than those computed for metallic alloys which is consistent with the lower values of cutting.

Although cutting forces values are significantly lower for polymers than for metallic parts, they are linked to the process stability and the final workpiece quality [10]. The prediction of cutting forces consequently remains a key aspect in the optimization of the cutting conditions and to obtain high quality parts, even though cutting forces are lower. Additionally, being able to predict a precise estimation of the cutting forces allows to manage the forces applied to the workpiece and to avoid its detachment from the building platform in the case of hybrid manufacturing [19].

The adjustment quality of the global approach can also be evaluated for each experimental test of the database (Table 3) using the performance indicator described in equation 5. Globally speaking, the RMS remains on the same order of magnitude as for the local optimization, apart from three cases (in grey in Table 3) showing a larger discrepancy between both approaches. For these outliers, the experimental cutting forces are significantly lower than most cutting forces measured during the other experimental tests. Since the model of the global approach is computed using the whole database, it makes sense for the simulation of these lower forces to be less accurate.

The advantage of using a physical model for regression allows having the adequate shape of the cutting force signal, even for cases where the identification is of a lower quality (Fig. 6).

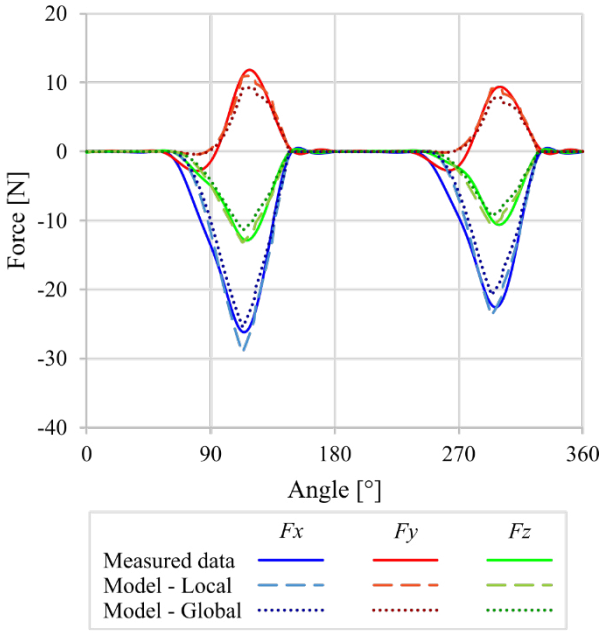

Fig. 6. Measured and modeled (local and global approaches) cutting forces along x, y and z directions for the f_z- case in dry conditions.

4. Conclusion and perspectives

This study investigated the milling behavior of 3D-printed PLA through an experimental plan that varied cutting speed, feed rate, and cutting fluid conditions (with and without air). Cutting forces were measured and analyzed to identify a linear cutting force model using an inverse approach. The proposed model demonstrated good agreement with experimental data, with a maximum RMS of 3.7 N for cutting force norms around 35 N. Therefore, this study showed that such model already used for metals is also applicable for polymer machining, no matter the cutting parameters.

Although the local linear model captures the overall trend, the identified coefficients exhibit significant variability across individual tests, highlighting the necessity of a global identification strategy. This global approach provides parameter estimates valid over the entire experimental domain, maintaining similar accuracy except for three outlier cases that show lower measured forces than the rest of the dataset. The global approach therefore enables the prediction of cutting forces across the experimental domain. Such predictive capability is essential to prevent workpiece detachment from the building platform during hybrid manufacturing operations.

Beyond the predictive capability enabled by the global approach, the model could offer a framework for assessing the influence of cutting conditions on force behavior, such as the effect of cutting fluid use on cutting coefficients or explaining the trends followed by the computed coefficients. Future work could also extend this method to non-linear models, incorporate

thermal and material removal mechanisms, and explore optimization strategies for improving the production of parts using a hybrid additive/subtractive approach. Furthermore, this model could be used to assess the influence of the anisotropy of FFF parts on the machining process.

References

[1] Pei E, Bernard A, Gu D, Klahn C, Monzón M, Petersen M, et al., editors. Springer Handbook of Additive Manufacturing. Cham: Springer International Publishing; 2023. https://doi.org/10.1007/978-3-031-20752-5.

[2] Gibson I, Rosen D, Stucker B, Khorasani M. Additive Manufacturing Technologies. Cham: Springer International Publishing; 2021. https://doi.org/10.1007/978-3-030-56127-7.

[3] Vyavahare S, Teraiya S, Panghal D, Kumar S. Fused deposition modelling: a review. Rapid Prototyp J 2019;26:176–201. https://doi.org/10.1108/RPJ-04-2019-0106.

[4] Mertkan İA, Tezel T, Kovan V. Improving surface and dimensional quality with an additive manufacturing-based hybrid technique. Int J Adv Manuf Technol 2023;128:1957–63. https://doi.org/10.1007/s00170-023-12055-z.

[5] Kalia S, Avérous L. Biodegradable and Biobased Polymers for Environmental and Biomedical Applications. John Wiley & Sons; 2016.

[6] Li Y, Wang S, Qian S, Liu Z, Weng Y, Zhang Y. Depolymerization and Re/Upcycling of Biodegradable PLA Plastics. ACS Omega 2024;9:13509–21. https://doi.org/10.1021/acsomega.3c08674.

[7] Kartal F, Kaptan A. EXPERIMENTAL DETERMINATION OF THE OPTIMUM CUTTING TOOL FOR CNC MILLING OF 3D PRINTED PLA PARTS. Int J 3D Print Technol Digit Ind 2023;7:150–60. https://doi.org/10.46519/ij3dptdi.1267634.

[8] Lalegani Dezaki M, Mohd Ariffin MKA. Post-processing of FDM 3D-Printed Polylactic Acid Parts by CNC Trimming. In: Dave HK, Davim JP, editors. Fused Depos. Model. Based 3D Print., Cham: Springer International Publishing; 2021, p. 195–212. https://doi.org/10.1007/978-3-030-68024-4_11.

[9] Cloëz L, Fontaine M, Gilbin A, Barrière T. Machinability of PLA obtained by injection molding under a dry milling process, 2024, p. 1877–86. https://doi.org/10.21741/9781644903131-208.

[10] Lorenzoni M, Spitaels L, Rivière-Lorphèvre E, Odent J, M'Saoubi R, Cloëz L, et al. Investigation on cutting fluid use in finish milling of polylactide (PLA) 3D-printed parts. Procedia CIRP 2025;133:656–61. https://doi.org/10.1016/j.procir.2025.02.112.

[11] Pămărac RG, Petruse RE. Study Regarding the Optimal Milling Parameters for Finishing 3D Printed Parts from ABS and PLA Materials. Acta Univ Cibiniensis Tech Ser 2018;70:66–72.

[12] Mehtedi ME, Buonadonna P, Carta M, Mohtadi RE, Marongiu G, Loi G, et al. Effects of milling parameters on roughness and burr formation in 3D- printed PLA components. Procedia Comput Sci 2023;217:1560–9. https://doi.org/10.1016/j.procs.2022.12.356.

[13] Arrazola PJ, Özel T, Umbrello D, Davies M, Jawahir IS. Recent advances in modelling of metal machining processes. CIRP Ann 2013;62:695–718. https://doi.org/10.1016/j.cirp.2013.05.006.

[14] Wan M, Li S-E, Yuan H, Zhang W-H. Cutting force modelling in machining of fiber-reinforced polymer matrix composites (PMCs): A review. Compos Part Appl Sci Manuf 2019;117:34–55. https://doi.org/10.1016/j.compositesa.2018.11.003.

[15] Engin S, Altintas Y. Mechanics and dynamics of general milling cutters.: Part I: helical end mills. Int J Mach Tools Manuf 2001;41:2195–212. https://doi.org/10.1016/S0890-6955(01)00045-1.

[16] Rivière-Lorphèvre E, Filippi E. Mechanistic cutting force model parameters evaluation in milling taking cutter radial runout into account. Int J Adv Manuf Technol 2009;45:8–15. https://doi.org/10.1007/s00170-009-1943-9.

[17] Rivière-Lorphèvre E, Van Hee M, Beuscart T, Ducobu F. Identification of Cutting Coefficients from Multiple Milling Tests. Procedia CIRP 2025;133:37–42. https://doi.org/10.1016/j.procir.2025.02.008.

[18] Insperger T, Mann BP, Stépán G, Bayly PV. Stability of up-milling and down-milling, part 1: alternative analytical methods. Int J Mach Tools Manuf 2003;43:25–34. https://doi.org/10.1016/S0890-6955(02)00159-1.

[19] Spitaels L, Aldeiturriaga Olabarri N, Bossu J, Martic G, Juste E, Rivière-Lorphèvre E, et al. Experimental evaluation of the maximal force before debonding a part from the build platform of an AM printer. vol. 41, Toulouse, France: Materials Research Forum LLC; 2024, p. 90–9. https://doi.org/10.21741/9781644903131-10.